

CHAPTER 18

Climate Research

Simon Blockley, Ian Matthews, Adrian Palmer, Ian Candy, Rebecca Kearney,
Pete Langdon, Catherine Langdon, Ashley Abrook, Paul Lincoln,
Amanda Farry, Chris Darvill and Laura Deeprise

Introduction

This chapter explores the analyses of records from a former lake, Lake Flixton, which allows us to reveal the local record of climatic and environmental change that is compared to the archaeological record in Chapter 9. While the general pattern of climate change for the North Atlantic and European region is known from records such as the Greenland ice cores (Chapter 4) it is essential to have a detailed understanding of records from nearby sites. This is partly because the expression of climate change is different regionally, but also for human groups it is the local environmental response to climate change that matters most. Fortunately for the Star Carr project, the site is located next to Lake Flixton; this is a natural archive for preserving past climatic and environmental data in the form of chemical changes to the lake water, pollen profiles that record changes in the local vegetation and insects that reflect different taxa with a range of temperature tolerances, which can in turn be used to reconstruct average temperatures. This chapter outlines the different methods used to examine the Lake Flixton record and summarises the main climatic and environmental changes that occurred during the period of Mesolithic human occupation in the area.

Methods

To establish the optimum location for extracting a palaeoenvironmental archive adjacent to the archaeological sites of Star Carr and Flixton Island, a detailed auger survey was undertaken. Dutch gouges, Russian corers and percussion drilling equipment were used to both record the base of the lake sediment sequences, and associated basal sediment types (Palmer et al. 2015). Russian corers and piston drilling equipment were then used to recover sediment that detailed the changing environments (Figure 18.1). The basin survey also suggested that there was significant variation in the topography of the basin and that only the deepest parts of the basin were likely to collect material from the very early period of deglaciation (Figure 18.2). Seven locations in the basin were sampled (Figure 18.2) and sections close to the Star Carr site (core B) had evidence of substantial marl formation suitable for more detailed analyses; further details of the sediment sequences can be found in Palmer et al. (2015).

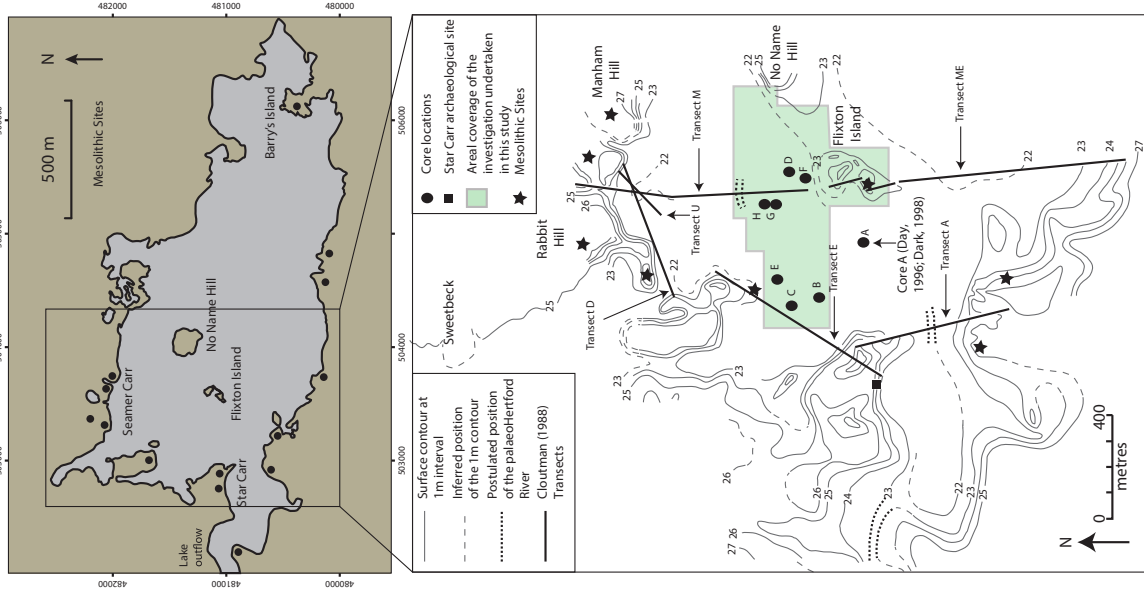
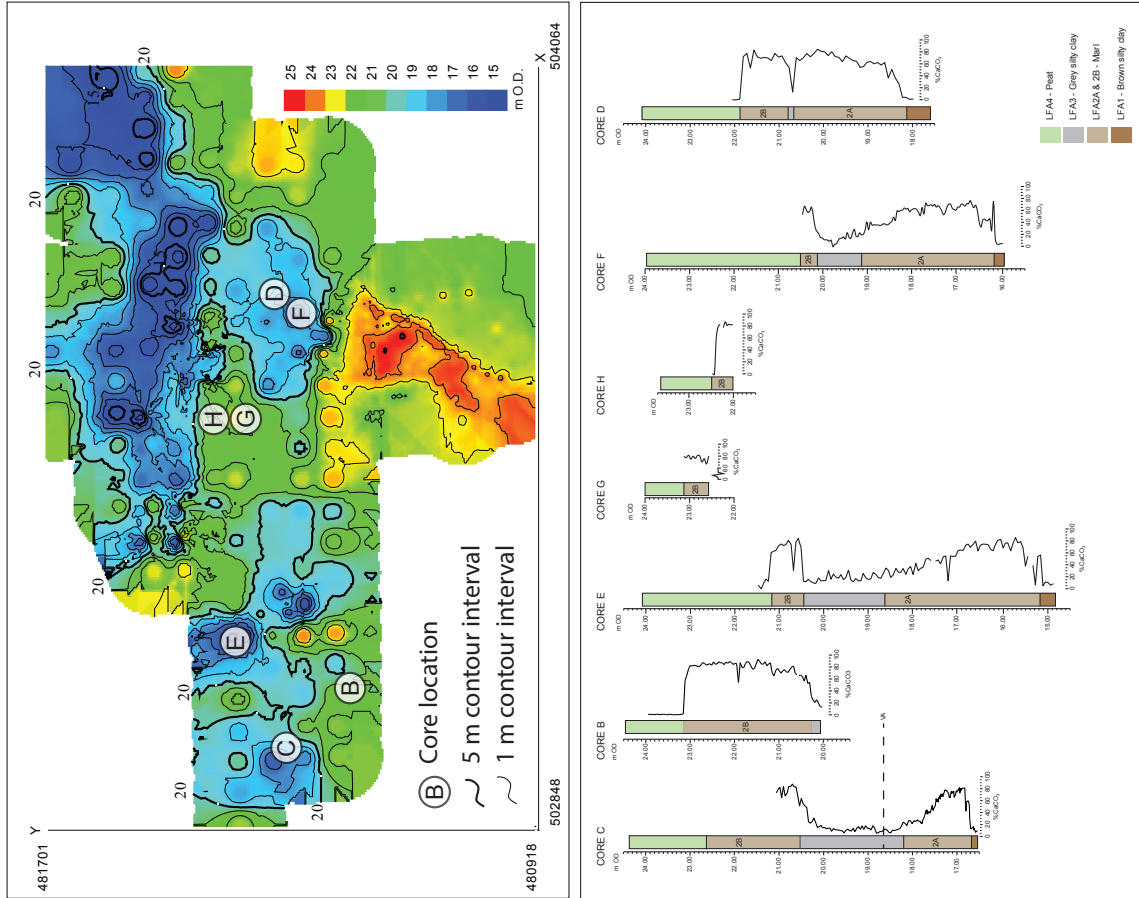
How to cite this book chapter:

Blockley, S., Matthews, I., Palmer, A., Candy, I., Kearney, R., Langdon, P., Langdon, C., Abrook, A., Lincoln, P., Farry, A., Darvill, C. and Deeprise, L. 2018. Climate Research. In: Milner, N., Conneller, C. and Taylor, B. (eds.) *Star Carr Volume 2: Studies in Technology, Subsistence and Environment*, pp. 113–121. York: White Rose University Press. DOI: <https://doi.org/10.22599/book2.d>. Licence: CC BY-NC 4.0



Figure 18.1: Piston coring of sediments in the deep lake sequence (core B from Palmer et al. 2015) used for palaeoenvironmental reconstruction in this chapter and detailed in Blockley et al. 2018) (Copyright Star Carr Project, CC BY-NC 4.0).

Figure 18.2 (page 115): Adapted from Figures in Palmer et al. (2015). Top left: Lake Flixton at its maximum extent with the location of major archaeological sites on the lake's margins. Bottom left: Location of key sites and contours for the eastern sector of Lake Flixton, including the location of the previous major bathymetric survey by Cloutman (1988a). The shaded area depicts the more detailed auger survey conducted by Palmer et al. (2015), which has been updated through subsequent work and extends the survey to the north. The results of this survey are presented (top right) with the major contours at 25, 20 and 15 m highlighted, allied to the position of the cores recovered during the course of this study. This depicts the likely topography immediately after the retreat of ice from the eastern Vale of Pickering characterised by a series of basins with different depths and area extents to the north of Flixton Island, which is the higher ground to the south of the study area. The evidence suggests that the distinctive palaeo-Hertford river channel as postulated by Cloutman (1988) does not exist. A summary of the stratigraphy in key cores recovered from the basins are presented in the figure to the bottom right. These demonstrate that there are often lake deposits which represent a series of abrupt climate shifts from the Dimlington Stadial (LFA 1), the relatively warm period of the Windermere Interstadial (LFA 2A), the abrupt cooling of the Loch Lomond Stadial (LFA 3) and the onset of the current Interglacial, the Holocene (LFA 4) (Reprinted from Palmer et al. 2015. Copyright (2015) with permission from Elsevier).



Borehole cores were opened in the laboratory and aligned using the stratigraphic overlaps to present the full lithostratigraphy of the record. They were then classified according to the Troels-Smith (1955) scheme. Subsamples were taken to account for the dominant stratigraphic layers in the core and, where possible, any sedimentary transitions. Basic sedimentological descriptions of the cores were supported by measurements of magnetic susceptibility, organic content, calcium carbonate content, particle size and pollen analysis. Sediment cores taken from close to Star Carr and Flixton Island revealed multiple coring locations with deep lacustrine sediments suitable for palaeoenvironmental analyses, and cores close to archaeological sites at Star Carr and Flixton Island were selected for further analyses. The cores closest to Star Carr (B and C) were analysed in the greatest detail and are discussed below.

The core material from boreholes close to Star Carr (Figure 18.2) was used to reconstruct the past climate at Star Carr through three major proxies: pollen, chironomids (non-biting midges) and stable isotopes. Samples of identified plant macrofossils were also picked for radiocarbon dating and age modelling of the sediments for comparison of the deep lake cores and the lake edge archaeological record. Additionally, the cores were also examined for the presence of cryptotephra to aid in the process of age modelling (see Blockley et al. 2018 and Palmer et al. 2015 for details of the radiocarbon and tephra analyses).

Pollen sampling was undertaken, in part to compare the stratigraphic record from the lake with previous studies but also with the vegetation record from monoliths taken through the archaeology (monolith M1 and the macrofossil and wood record from Star Carr). Pollen samples were taken with a 1 cm³ volumetric sampler washed, deflocculated in sodium pyrophosphate and sieved at 125 and 15 microns before extraction using heavy liquid separation. Samples were spiked with *Lycopodium* spores to allow for quantification of pollen concentration and analysed using a research grade biological microscope (full details are available in Blockley et al. 2018). Samples for the study of macrofossil plant remains were disaggregated and sieved to 0.3 mm, avoiding the use of any organic chemicals where material is likely to be needed for dating. They were examined using low-power reflected light and transmitted light microscope.

Chironomid larvae occupy a large range of aquatic habitats and they are found in most freshwater environments. The larvae possess a chitinous head capsule, which is shed at various stages of development. The head capsules from the 3rd and 4th instars (developmental stages) are typically preserved in lake sediments as fossils, and hence can be extracted from the sediments and typically identified to genus or species morphotype. This allows the past chironomid fauna to be reconstructed and chironomids have long been shown to be excellent indicators of temperature as this influences their emergence, flight, swarming, maturing of eggs and sexual activity (Pinder 1986). Many studies have documented the influence of temperature on chironomid distribution and how they can be used to reconstruct past summer temperatures (e.g. summaries in Brooks 2006; Walker & Cwynar 2006). Sediment samples for chironomids (usually ~2 cm³ wet weight) were disaggregated in 10% KOH and then sieved to remove the small particles <90 µm, whilst retaining all head capsules. The samples were next placed in a sorting tray where chironomid head capsules were picked out using fine forceps. The head capsules were mounted on microscope slides in Hydro-Matrix and identified under ×400 magnification. Current subfossil chironomid taxonomy is based on Brooks et al. (2007). A total of 122 chironomid samples were analysed from Star Carr core B and C covering the Early Holocene and Loch Lomond stadial transition (the Loch Lomond Stadial is the British term for a cooling event at the end of the Late Glacial that broadly equates to the Younger Dryas in continental Europe and Greenland Stadial 1). The sample data were analysed using a transfer function for summer temperatures developed from Norwegian lakes (Brooks and Birks 2001), which yielded quantitative summer temperature reconstructions.

In addition to chironomid analyses parallel samples were taken for isotopic analyses of lake carbonates. The δ¹⁸O value of lacustrine carbonate is primarily controlled by 1) the temperature at which carbonate mineralisation occurs and 2) the δ¹⁸O value of the lake water. The second factor is determined by the δ¹⁸O of rainfall which is controlled by a range of factors, including air temperature, amount of rainfall, seasonality of rainfall and distance from the moisture source (Rozanski et al. 1992; Rozanski et al. 1993; Darling 2004). Stable carbon isotopic ratios reported as δ¹³C are determined by a range of factors in a lake setting including the amount of organic input and productivity in a lake, and, at this site, also inwash of minerogenic carbonate from the surrounding chalk. The latter is an indicator of a detrital component to the lake record and we have excluded any paired isotope samples where the carbon isotope δ¹³C value rises above 2, as this is close to the value of the surrounding bedrock (see Blockley et al. 2018). A total of 200 isotope samples were taken from the Star Carr core B over sediment bedrock depth 2 to 5 m below current soil surface; approximately 20–23 m OD, with the period covering the Early Holocene (2–3 m) analysed in greatest detail and 26 samples were taken from core C between 2.83 m

and 4 m depth in core (c. 21 to 19.83 m OD). Carbonate samples for oxygen and carbon isotopic analyses were sampled at 10 mm, disaggregated in sodium hexametaphosphate and sieved over a 63 micron mesh with the greater than 63 micron fraction used for further analyses. The remaining sample was treated with hydrogen peroxide to remove organics, weighed in a microbalance, and oxygen and carbon isotopes were measured on the liberated fraction of CO₂ after reaction with phosphoric acid at 90°C. Isotopic measurements are reported with reference to VPDB standard (Blockley et al. 2018).

Results

Auger survey

The transect auger survey and the detailed deep coring results are presented in Figure 18.2 (adapted from Palmer et al. 2015). The surface topography outlined in Figure 18.2 represents the deepest measured position where the base of the auger reached glacial deposits, measured relative to current sea level. These reveal a series of small isolated basins within the lake topography, consistent with kame and kettle topography often associated with deglaciated landscapes.

Analyses of the basal sediments recorded in the augers was also compared to the detailed stratigraphy of sediments analysed from cores extracted using Russian corers and mechanical coring. These detailed cores (Figure 18.2) show brown and grey silty clays, and marls, all overlain by peat deposits. These are also compared to magnetic susceptibility measurements and calcium carbonate concentrations. These deposits relate to different processes of deposition in the lake and can be taken broadly to indicate key time periods in the evolution of the lake from basal brown clay sediments, laid down in the early postglacial environment, with two phases of marl deposition during warmer conditions, separated by grey clays marking a cold reversal. This depositional sequence has been interpreted as marking the succession from early Interstadial marl and carbonate rich sediments, Loch Lomond Stadial clays and Holocene marls and peat. Combining these data with the basin survey has led to a model of changing hydrology in the lake suggesting that the lake fluctuated in size and depth over time, linked to changes in the wider environment. In particular the study suggested that water levels dropped during the Loch Lomond Stadial and then rose into the Early Holocene.

Palaeoenvironmental and palaeoclimatic records

The chironomid inferred temperature and $\delta^{18}\text{O}$ and $\delta^{13}\text{C}$ results from the detailed palaeoclimate study of borehole B from the transect survey are presented in Figure 18.3. This record has marl accumulation from 21.1 m to 20.2 m OD (2 m to 5.2 m below ground surface). A dip in calcium carbonate values and a thin clay layer at 3 m (21.9 m OD) is thought to represent a hiatus in sedimentation at this point in the core due to lowering of the water table during the Loch Lomond Stadial. Thus this core captures environmental and climatic conditions during both the Late Glacial Interstadial and Early Holocene (the transition is marked on Figure 18.3 at a core depth of 3 m). The data to the left of the line marked 'hiatus' is the section covering Early Holocene sedimentation in this record, although it is likely that in this core there is a lag between the start of the Holocene and the start of sedimentation, due to the OD height of the core and the time taken for the water table to rise after the Loch Lomond stadial. Interestingly, however, in this record it seems that in terms of both isotopic ratios and chironomid inferred temperatures the climate conditions in the Early Holocene are similar to those during the Late Glacial Interstadial.

Due to this hiatus, further investigation was undertaken on the transition between clay and marl from 3 m to 5 m in core C (Figure 18.2). This core was known to have a much more extensive record of Loch Lomond stadial sedimentation and is located deeper in the basin, and is thus less likely to have been cut off from sediment supply during periods of low lake level in the Loch Lomond stadial. In addition, this core was known to contain the Vedde Ash tephra, dating to the mid Loch Lomond stadial at a depth of 5.26 m (Palmer et al. 2015), demonstrating sedimentation during the mid Loch Lomond stadial in the form of grey silts and clays that shift to marl formation at 21.5 m OD. As with core B this core was analysed for chironomids and $\delta^{18}\text{O}$ and $\delta^{13}\text{C}$, and these are detailed in Figure 18.4. Finally, both cores have detailed pollen profiles for comparison with the lake records. These are shown in full in Blockley et al. (2018), but summary pollen data is also shown in Figures 18.5 and 18.6.

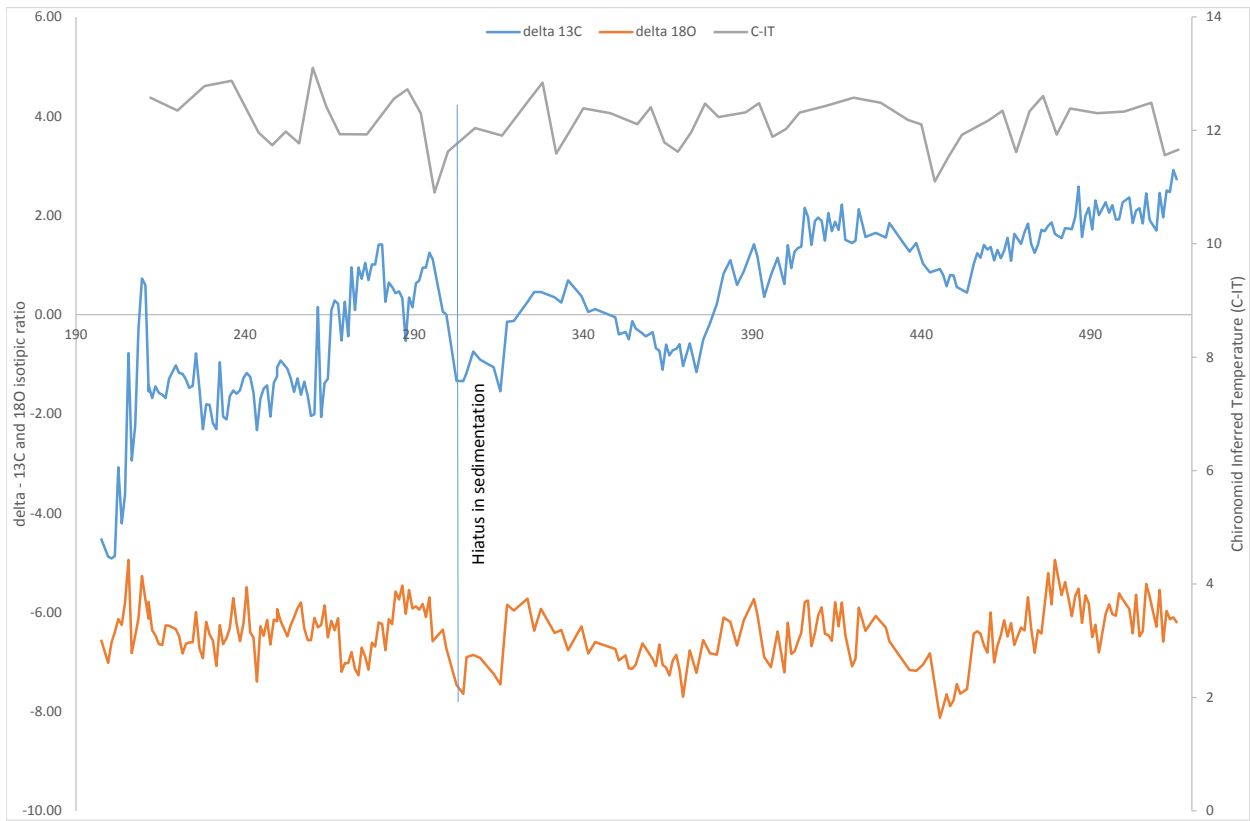


Figure 18.3: Chironomid inferred temperatures and $\delta^{18}\text{O}$ from core B, close to Star Carr. The x-axis provides depth of sediment within the core: the position at 3 m core depth marks the hiatus in the record during the Loch Lomond stadial/Early Holocene (Copyright Star Carr Project, CC BY-NC 4.0).

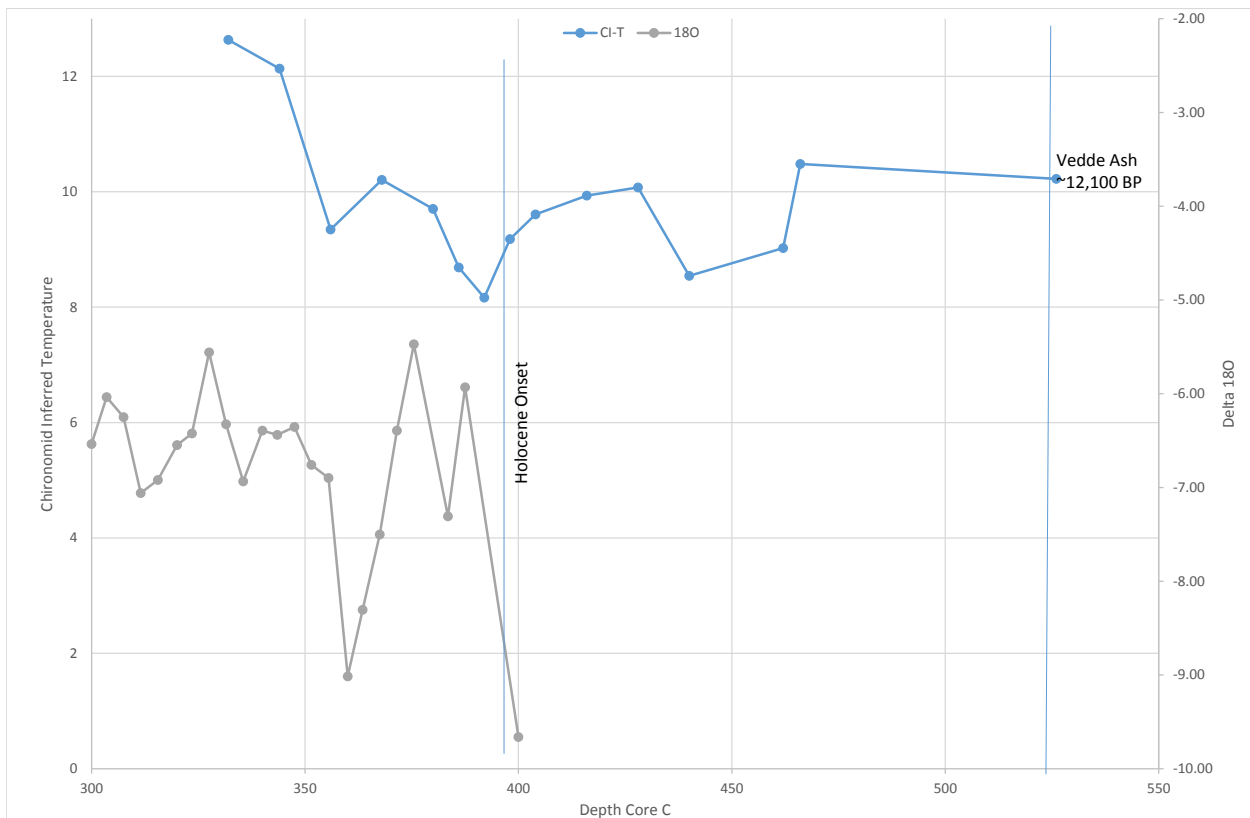


Figure 18.4: Chironomid inferred temperatures (CI-T) and $\delta^{18}\text{O}$ from core B covering the Loch Lomond stadial to Holocene boundary and showing the baseline values around the Vedde ash tephra (Copyright Star Carr Project, CC BY-NC 4.0).

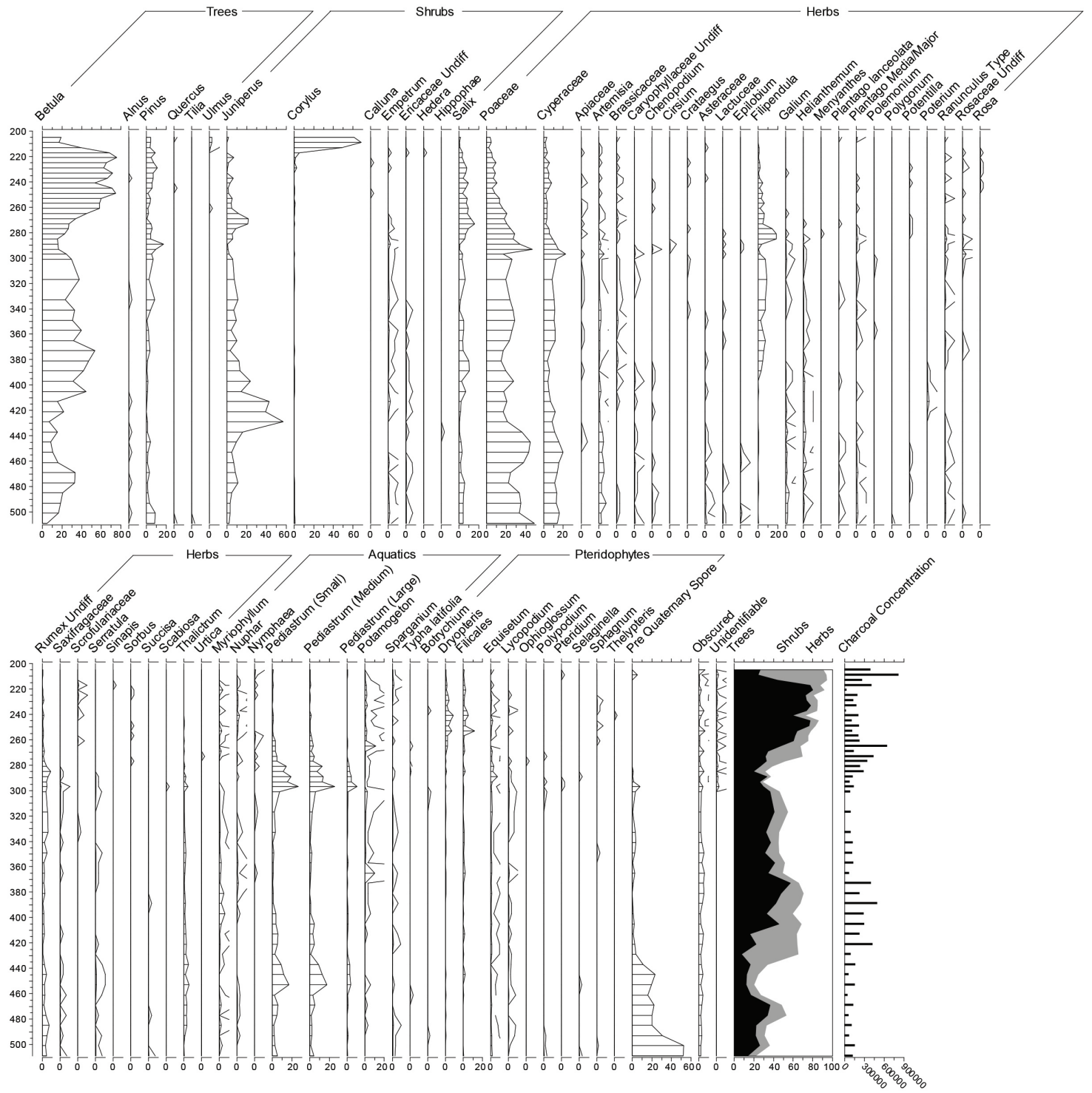


Figure 18.5: Core B percentage pollen taxa (Copyright Star Carr Project, CC BY-NC 4.0).

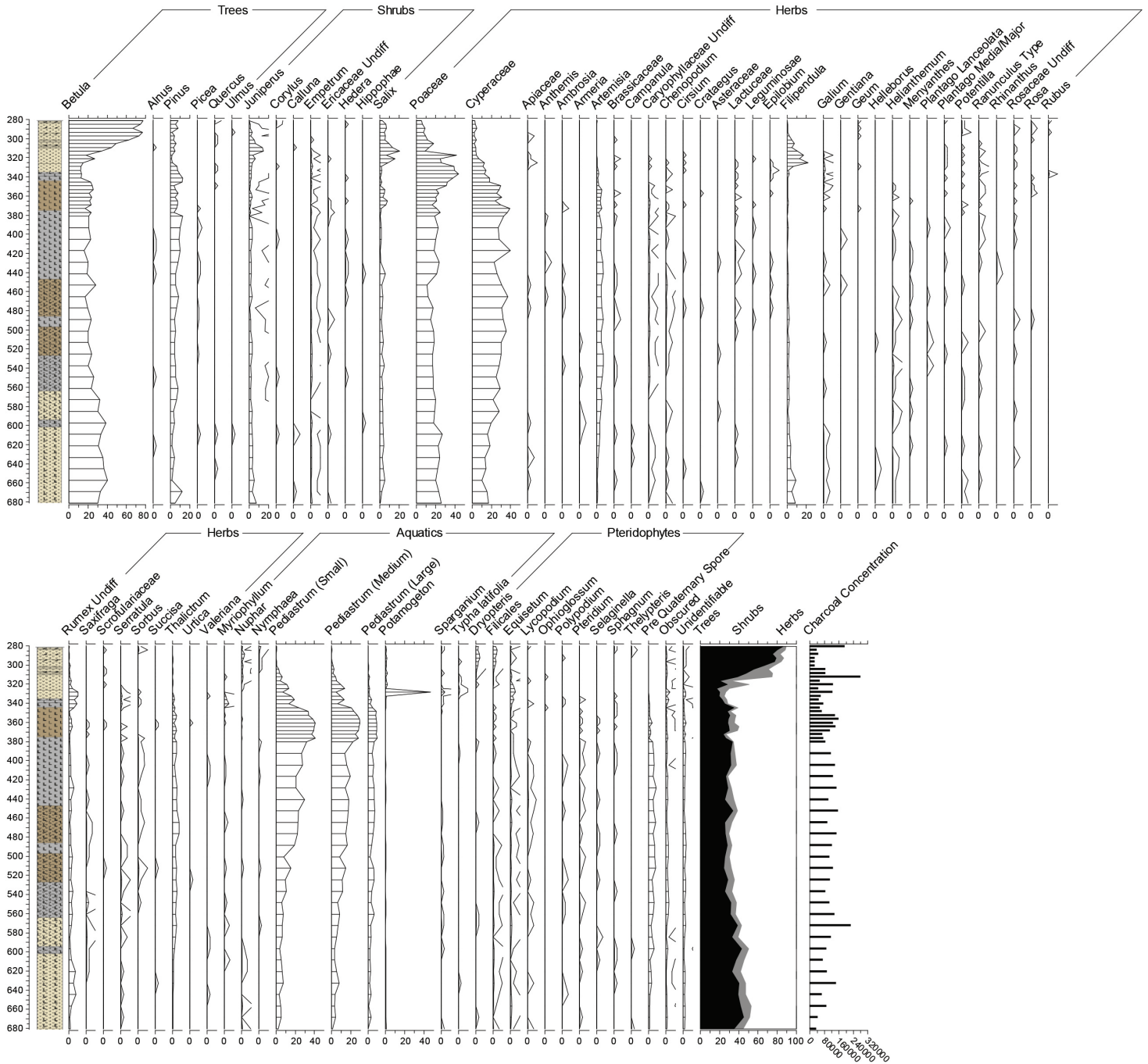


Figure 18.6: Core C percentage pollen taxa (Copyright Star Carr Project, CC BY-NC 4.0).

In core B the palaeotemperature proxies show a shift out of Loch Lomond stadial conditions at a depth of 3.87 to 3.85 m below ground surface, with a sharp shift in the oxygen isotopes, but more muted shift in chironomids, suggesting that summer temperatures at the start of the Holocene were still not significantly above the baseline Loch Lomond stadial conditions seen in the values around the time of the Vedde ash at 5.26 m. The Early Holocene continues to be unstable in these cores with fluctuations at 3.75 m and 3.56 m. In core B

the chironomid inferred temperatures and $\delta^{18}\text{O}$ values also indicate a fluctuating Early Holocene climate after the onset of Holocene sedimentation in this core. The $\delta^{18}\text{O}$ shows shifts of -2 per mille from initial Holocene warming just after 3 m to the first of several Early Holocene troughs. These values are equivalent to fluctuations in $\delta^{18}\text{O}$ seen in the preceding Late Glacial and these are mirrored by temperature fluctuations of c. 2°C in the chironomid record, again consistent with Late Glacial values.

In order to compare these data to the archaeological record of Star Carr and nearby Flixton Island (where Long Blade archaeological material has been located) the cores were radiocarbon dated. These dates, along with tephra information, were incorporated into a Bayesian sequence model (Blockley et al. 2018) and this was tied into the Star Carr environmental monolith record using common pollen taxa changes found in both cores. The details of this, along with their relationship to the archaeology of the area, are discussed in detail in Chapter 9.

Conclusions

This work has combined a range of palaeoenvironmental indicators taken from lake boreholes close to the Star Carr site. The advantage of this approach is that it has allowed the climatic and environmental signal close to the area of human occupation to be examined in detail. These environmental records suggest that around the time of human occupation of Star Carr there were significant climatic fluctuations, beginning with the shift out of the cold preceding stadial, but with two further shifts in Early Holocene climate. These transitions, identified in a range of proxies are the backdrop for the human occupation of the site and are discussed alongside the archaeological record in Chapter 9.

